Journal of Science: Advanced Materials and Devices 1 (2016) 351–361

Contents lists available at ScienceDirect

Journal of Science: Advanced Materials and Devices

journal homepage: www.elsevier.com/locate/jsamd

Original Article

Processing and characterization of polystyrene nanocomposites based on Co–Al layered double hydroxide

Kelothu Suresh, R. Vinoth Kumar, G. Pugazhenthi*

Department of Chemical Engineering, Indian Institute of Technology Guwahati, Guwahati 781039, Assam, India

ARTICLE INFO

Article history:
Received 25 June 2016
Received in revised form
23 July 2016
Accepted 23 July 2016
Available online 29 July 2016

Keywords:
Polystyrene
Layered double hydroxides
Nanocomposites
Kinetic
Rheology

ABSTRACT

The present work deals with the development of polystyrene (PS) nanocomposites through solvent blending technique with diverse contents of modified Co–Al layered double hydroxide (LDH). The prepared PS as well as PS/Co–Al LDH (1–7 wt.%) nanocomposites were characterized by X-ray diffraction (XRD), transmission electron microscopy (TEM), Fourier transform infrared spectroscopy (FTIR), rheological analysis, thermogravimetric analysis (TGA) and differential scanning calorimetry (DSC). The XRD results suggested the formation of exfoliated structure, while TEM images clearly indicated the intercalated morphology of PS nanocomposites at higher loading. The presence of various functional groups in the Co–Al LDH and PS/Co–Al LDH nanocomposites was verified by FTIR analysis. TGA data confirmed that the thermal stability of PS composites was enhanced significantly as compared to pristine PS. While considering 15% weight loss as a reference point, it was found that the thermal degradation (T_d) temperature increased up to 28.5 °C for PS nanocomposites prepared with 7 wt.% Co–Al LDH loading over pristine PS. All the nanocomposite samples displayed superior glass transition temperature (T_g), in which PS nanocomposites containing 7 wt.% LDH showed about 5.5 °C higher T_g over pristine PS. In addition, the kinetics for thermal degradation of the composites was studied using Coats-Redfern method. The Criado method was ultimately used to evaluate the decomposition reaction mechanism of the nanocomposites. The complex viscosity and rheological muduli of nanocomposites were found to be higher than that of pristine PS when the frequency increased from 0.01 to 100 s^{-1}.

1. Introduction

Layered double hydroxides (LDHs) are well characterized anionic clays and utilized in wide range of technological application such as catalysts, adsorbents, separation techniques and ion-exchangers [1]. The general chemical formula of LDH is $[M^{2+}_{1-x}\ M^{3+}_{x}(OH)_2]^{x+}(A^{n-})_{x/n}.mH_2O$, where, M^{2+} is a metal divalent cations (Co^{2+}, Mg^{2+}, Zn^{2+}, Ni^{2+}), M^{3+} is a metal trivalent cations (Mn^{3+}, Ga^{3+}, Al^{3+}, In^{3+}) and A^{n-} is an interlayer anions (NO_3^-, Cl^-, CO_3^{2-}, OH^-). LDH consists of closely filled hydroxyl anion planes, which lie on top of triangular lattice. The inter layer spacing of LDH contains both water molecules and interlayer anions. There is an intricate arrangement of hydrogen bonds between anions, water molecules and layered hydroxyl groups [2]. The recent progress in polymer/layered nanocomposites (PLNs) has been the most important mile stone achievement in the polymer technology [1–3]. The PLNs have been used in various applications due to their superior thermal, mechanical and fire retardant properties over pristine polymer, [3].

The polymer nanocomposite can be prepared by several methods, including melt compounding [4], emulsion polymerization [5], in-situ polymerization [6], and solvent blending method [7]. The solvent blending technique is widely used and it consistently gives exfoliated nanocomposites [7]. The preparation of various types of polymer nanocomposites was reported in numerous literatures [8–15]. Liu et al. [8] synthesized Co–Al LDH using various anions (acetate, chlorate and nitrate), and found that the NO_3-LDH gives greater degree of exfoliation as compared to other modifiers. Guo et al. [9] prepared polyurethane (PU)/Co–Al LDH composites by in-situ polymerization technique. They reported that the decomposition temperature of PU/Co–Al LDH nanocomposite with 5 wt.% LDH was found to be 36.4 °C lower than the pristine PU. Qiu et al. [10] incorporated Zn–Al LDH nanoparticle in the PS matrix by solution intercalation method. They reported that the thermal decomposition temperature of the nanocomposites is 17 °C more than that of pristine PS. In another study,

* Corresponding author. Fax: +91 361 2582291.
E-mail address: pugal@iitg.ernet.in (G. Pugazhenthi).
Peer review under responsibility of Vietnam National University, Hanoi.

http://dx.doi.org/10.1016/j.jsamd.2016.07.007

Paul et al. [11] also prepared PS/O-laponite nanocomposites using solution intercalation technique and attained improvement in the thermal stability (425 °C for pristine PS and 454 °C for PS/O-laponite composites) due to the presence of O-laponite in PS matrix. PS/Mg Al LDH nanocomposites containing 5 wt.% LDH prepared by in-situ free radical bulk polymerization method displayed about 18 °C enhancement in thermal stability over pristine PS [12]. A simple solution intercalation technique was adopted for the preparation of polycaprolactone/Co–Al LDH nanocomposites [13]. TGA result clearly demonstrated that the nanocomposites had around 18 °C lower thermal degradation temperature as compared to pure polycaprolactone [13]. Recently, Kumar and co-workers [14] investigated the effects of Co–Al LDH concentrations on the properties of poly(methyl methacrylate) (PMMA) nanocomposites which were prepared by solvent blending method. They reported that the PMMA/Co–Al LDH nanocomposites with 7 wt.% LDH exhibited improved thermal stability (25 °C) over pristine PMMA. Limpanart et al. [15] followed melt compounding technique to synthesis PS/clay nanocomposites. They observed that two major types of composites namely, conventional and intercalated nanocomposites obtained depending on the modification of the organoclay. Zang et al. [16] synthesised PS/clay nanocomposites by γ-ray irradiation technique. They found that the incorporation of clay greatly improved the thermal properties of the PS nanocomposites. The formation of exfoliated PS/clay nanocomposites via in-situ polymerization was demonstrated by Uthirakumar et al. [17]. They reported that a delaminated structure was obtained due to the anchored radical initiator within the clay layers. Chen and Wang [18] prepared polypropylene (PP) composites by melt blending method and studied the thermal decomposition kinetics of the nanocomposites. They utilized Coats-Redfern and Criado model to measure the activation energy and determine the reaction mechanism of PP nanocomposites, respectively.

It is worth to point out that the most of the earlier studies on polymer nanocomposites was based on montmorillonite type of layered silicate clays. In recent years, LDHs have been considered as efficient nanofiller for the preparation of PS nanocomposites due to its tunable properties and higher chemical purity. Moreover, polymer nanocomposites containing exfoliated LDH possessed more exfoliated clay layers as compared to layered silicate based polymer nanocomposite [19,20]. In this work, a facile route (solvent blending) is chosen for the synthesis of PS/Co–Al LDH nanocomposites containing different concentrations of Co–Al LDH. The effect of LDH content (1–7 wt.%) on the structural, thermal and rheological behavior of PS nanocomposite films is examined. The thermal degradation kinetics and reaction mechanisms of the nanocomposites are also investigated.

2. Experimental

2.1. Materials

PS was acquired from National Chemicals Ltd., (Gujarat) India. Cobalt nitrate ($Co(NO_3)_2 \cdot 6H_2O$), aluminium nitrate ($Al(NO_3)_3 \cdot 9H_2O$), xylene (C_8H_{10}), sodium hydroxide (NaOH) and sodium dodecyl sulfate (SDS) were procured from Merck (I) Ltd., Mumbai, India. Water used for this work was taken from the Millipore water system (ELIX-3).

2.2. Synthesis of organomodified Co–Al LDH

Co–Al LDH was prepared using SDS through co-precipitation method by following the procedure described elsewhere [21]. Initially, Cobalt nitrate, aluminium nitrate and SDS were dispersed in water (500 mL) to form a solution containing Co^{2+}/Al^{3+}/SDS with a desirable molar composition (2:1:1.5). An aqueous solution of 2 M NaOH was further added drop by drop, which was accompanied by dynamic stirring until to reach pH 8.5. Then, it was stirred for 16 h to form precipitate at ambient conditions. The thick slurry was collected on top of the filter paper during the filtration of the precipitated solution. Finally, the precipitate was washed with water until the pH of the residual filtrate becomes neutral. This final purified product was kept in the atmospheric condition for 12 h and consecutively dried at 70 °C for 16 h in a hot air oven. Then the obtained Co–Al LDH powder was utilized for the preparation of PS nanocomposites.

2.3. Synthesis of PS/Co–Al LDH nanocomposites

PS/Co–Al LDH nanocomposites were synthesized by solvent blending process using xylene as a solvent. Initially, Co–Al LDH and PS were dried at 70 °C and 60 °C, respectively, for 12 h in a hot air oven to remove the moisture content. A required quantity of Co–Al LDH (see Table 1) was weighed and dispersed in 109 mL of xylene and continuously stirred for 24 h. The requisite amount of PS was added to Co–Al LDH solution after 24 h of continuous stirring, followed by 12 h of stirring of the PS/Co–Al LDH solution. The resulting solution was poured on a flat Petri dish and kept it for 16 h at ambient conditions. Finally, the film was heated around 60 °C to eliminate the residual solvent to get PS/Co–Al LDH nanocomposite. A clean PS sample (without Co–Al LDH) was also prepared in a same manner. To study the influence of LDH content on the morphological, thermal and rheological behavior of the prepared PS nanocomposites, PS/Co–Al LDH nanocomposites were prepared with different weight loadings (1, 3, 5, and 7 wt.%) of LDH. Note that, all the compositions are designated as pristine PS, PS 1, PS 3, PS 5 and PS 7 for pure polystyrene, PS/Co–Al LDH 1(wt%), PS/Co–Al LDH 3 (wt%), PS/Co–Al LDH 5 (wt%), and PS/Co–Al LDH 7 (wt%), respectively. The experimental procedure used for synthesis of nanocomposites is schematically presented in Fig. 1.

2.4. Characterization

The interlayer distance of various PS/Co–Al LDH nanocomposites were primarily investigated by XRD analysis. The XRD profiles were recorded using X-ray diffractometer (Make: Bruker, Model: D8 ADVANCE) with Cu-Kα radiation and Ni filter at room temperature. Further, the structural morphology of the nanocomposites was done using transmission electron microscopy (TEM) (Make: JEOL, Model: JEM 2100) operated at 200 kV. Fourier transform infrared (FTIR) spectroscopy (Make: Shimadzu, Model: IR Affinity-1) was employed to identify the existence of LDH in the PS matrix and different functional groups present in the LDH in the wave length ranging between 4000 and 400 cm^{-1}. In order to assess the thermal stability of the nanocomposites, TGA was done under nitrogen atmosphere using high temperature thermogravimetric system (Make: Mettler Toledo, Model: TGA 851e/LF/1100). The heating ramp was maintained at 10 °C/min in the temperature

Table 1
Preparation chart for PS/Co–Al LDH nanocomposites.

Sample	LDH Loading (wt.%)	LDH (g)	PS (g)	Solvent (mL)
PS	0	0	5	109
PS 1	1	0.05	4.95	109
PS 3	3	0.15	4.85	109
PS 5	5	0.25	4.75	109
PS 7	7	0.35	4.65	109

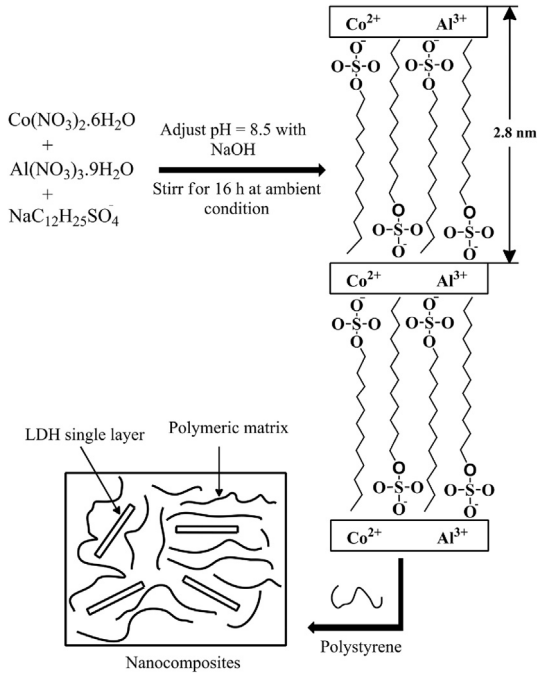

Fig. 1. Flowchart for the preparation of modified Co–Al LDH and PS/Co–Al LDH nanocomposites.

range of 30–700 °C for all the samples. The DSC measurements were performed using an instrument (Make: Mettle Toledo, Model: 1) with acquisition ranging from 25 °C to 200 °C at a heating rate of 5 °C/min. The rheological characteristics of the nanocomposites samples were determined using Rheometer (Make: Anton Paar; Model: MCR 301) with oscillation mode at temperature of 190 °C. Parallel plate geometry (50 mm diameter disc, 1 mm of thickness) was employed for the analysis.

3. Results and discussion

3.1. XRD analysis

The structural properties of the nanocomposites are highly influenced by the degree of dispersion of LDH in the PS matrix. When layered nanofillers used as reinforcing material, generally either intercalated or exfoliated structure are formed. This primarily depends on the synthesis method, content of the filler and chemical nature of the organic modifier used in the filler. If an intercalated composite is formed, there will be an increment in the d-spacing value as compared to original LDH. The exfoliated nanocomposite is produced when the LDH layers are well separated from one to another and well distributed in the polymer and no peak corresponding to basal plan (003) of LDH is observed. Generally, in the polymer/clay nanocomposite systems, the state of dispersion and the interlayer spacing of the clay platelets are typically examined by XRD and TEM. TEM is time demanding, and merely provides qualitative information on the sample in total, whereas XRD gives quantification of changes in layer spacing, however, without providing information on high layer spacing (>7 nm) and/or relatively disordered structures. Hence, both these techniques (XRD and TEM) are generally used to assess the nanocomposite structures [22]. Fig. 2 shows the XRD results of Co–Al LDH, PS and PS nanocomposites in the 2θ range of 2°–50° with a scan speed of 0.02 s^{-1}. The d-spacing value of the Co–Al LDH is determined as 2.8 nm from the reflection peak (003) at 3.14°

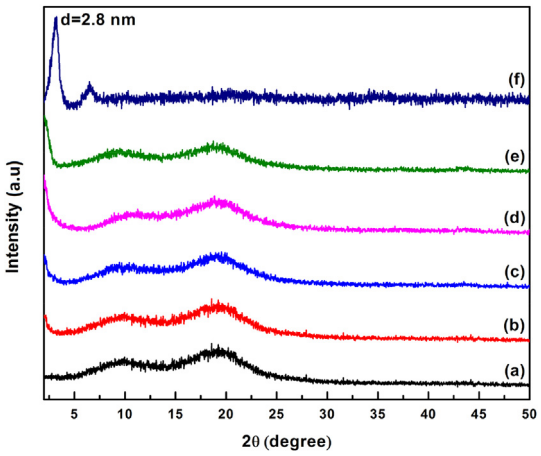

Fig. 2. XRD patterns of (a) pristine PS, (b) PS 1, (c) PS 3, (d) PS 5, (e) PS 7 and (f) Co–Al LDH.

through Bragg's equation, $d = n\lambda/2\sin\theta$; here, $\lambda = 1.5406$ Å and $n = 1$. In Fig. 2 (b–e), the characteristic peak (003) of Co–Al LDH layers is completely disappeared in the PS nanocomposites suggesting that LDH layers might be exfoliated or delaminated in the PS matrix. As mentioned, XRD technique alone is not sufficient to conclude the kind of nanocomposite structures formed and it should be used together with TEM to obtain the assessment of dispersion [22].

3.2. TEM analysis

TEM is more useful technique for evaluating the distribution of LDH in the polymer matrix as compared to XRD and FESEM techniques [22]. TEM images of PS1, PS 3, PS 5 and PS 7 nanocomposites are presented in Fig. 3 (a–d). The TEM images can provide a qualitative understanding of dispersion of the LDH and the type of nanocomposites formed, i.e., intercalated or exfoliated. One can see from Fig. 3 (a–b) that in the case of PS 1 and PS 3 samples, a better dispersion of Co–Al LDH layers in PS matrix is noticed. The dark lines show the LDH galleries and the bright region signifies the PS matrix. These images (Fig. 3 (a) and (b)) indicate that the LDH layers have lost their ordered stacking structure, and are totally delaminated in the PS matrix. The galleries lines are illustrated by arrow marks. However, the PS nanocomposite with 5 wt.% Co–Al LDH is found to have partially exfoliated and intercalated structure (see Fig. 3 (c)). The arrow and circle marks represent the exfoliated and intercalated structure, respectively. Fig. 3(d) illustrates the intercalated morphology of PS nanocomposites at higher loading of LDH (7 wt.%) in the PS matrix. A similar behavior was also reported for PS/Mg–Al LDH nanocomposites prepared by solution intercalation route [6]. Based on the attained results, it can be confirmed that the delaminated PS/LDH nanocomposites are formed at lower loading of nanofiller (<3 wt.%).

3.3. FTIR analysis

A typical FTIR spectrum of Co–Al LDH, pristine PS and PS 5 nanocomposite is illustrated in Fig. 4. Apparently, for Co–Al LDH sample (Fig. 4 (a)), the medium sharp peak at 1063 cm^{-1} and an intense peak at 1218 cm^{-1} are designated as asymmetric and symmetric vibration of sulfate from dodecyl sulfate anion, respectively [14]. The characteristic peaks at 2957 cm^{-1}, 2920 cm^{-1} and 2848 cm^{-1} are ascribed to C–H stretching vibration. Bending mode of water molecule is found through a prominent peak at 1630 cm^{-1}.

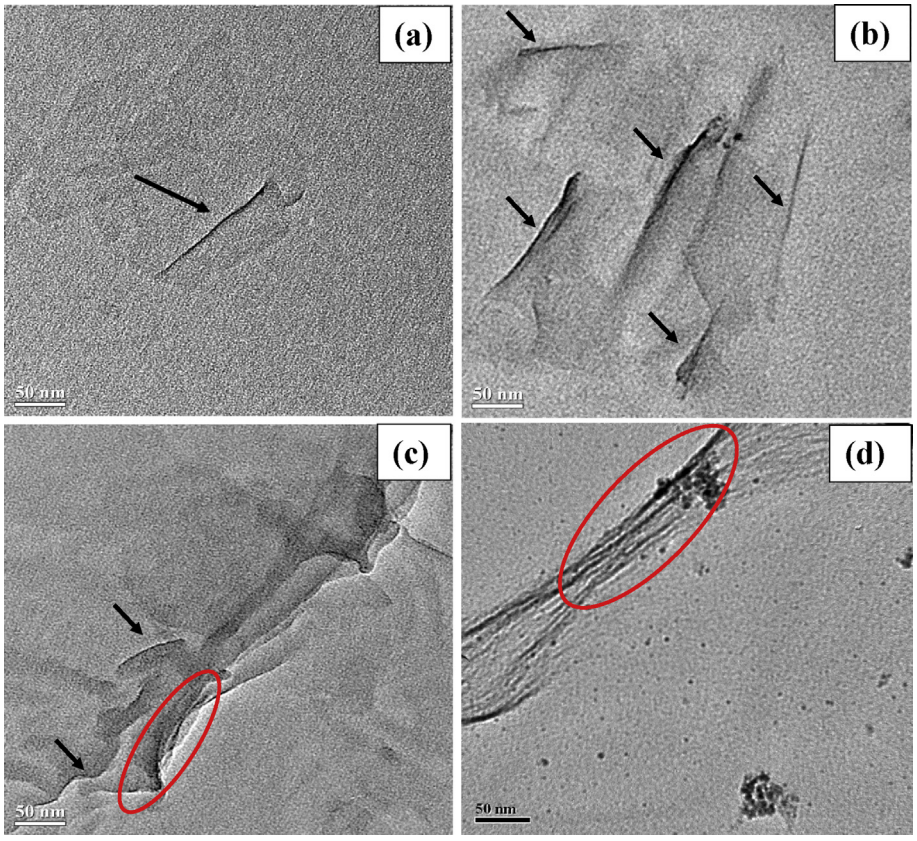

Fig. 3. TEM images of (a) PS 1, (b) PS 3, (c) PS 5 and (d) PS 7 nanocomposites.

A very strong and broader peak attained at 3500 cm^{-1} is attributed to the O–H stretching of the metal hydroxide layer and interlayer water molecules of Co–Al LDH. For pristine PS sample (Fig. 4 (b)), an intense peak is appeared at 698 cm^{-1}, which is assigned as mono substituted benzene. Vibrational mode of CH_2 bending is located at 1453 cm^{-1} and 1368 cm^{-1}. There is two peak appeared at 1504 cm^{-1} and 1496 cm^{-1} that are designated as C=C bending vibration [21]. The medium sharp peak at 2930 cm^{-1} and 3070 cm^{-1} correspond to aliphatic C–H stretching vibration and aromatic C–H stretching vibration, respectively. In comparison with pristine PS sample (Fig. 4(b)), PS 5 nanocomposite (Fig. 4(c)) shows few new additional absorption prominent peaks; one is at 1218 cm^{-1} that corresponds to symmetric vibration of sulfate from dodecyl sulfate anion, another one located at 1630 cm^{-1} is assigned to bending mode of water molecules and a broader peak attained at 3500 cm^{-1} indicates the existence of O–H stretching modes of interlayer water molecules. These peaks elucidate the occurrence of Co–Al LDH in the PS nanocomposites. When the content of Co–Al LDH increases in the PS matrix, the intensities of LDH bands lead to be stronger in the FTIR spectra (Fig. 5). Wang et al. [23] also obtained similar results with increasing the loading of MMT on polymer nanocomposites.

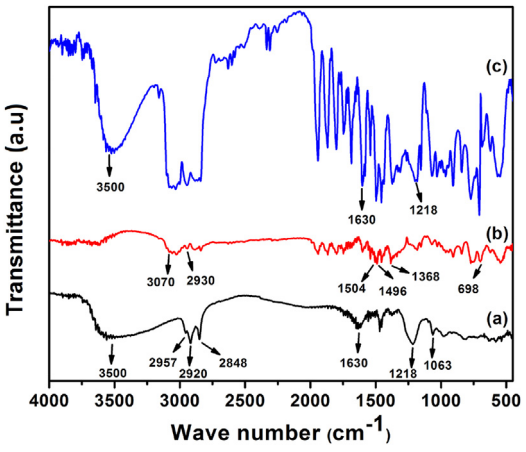

Fig. 4. FTIR spectrum of (a) Co–Al LDH, (b) pristine PS and (c) PS 5 nanocomposite.

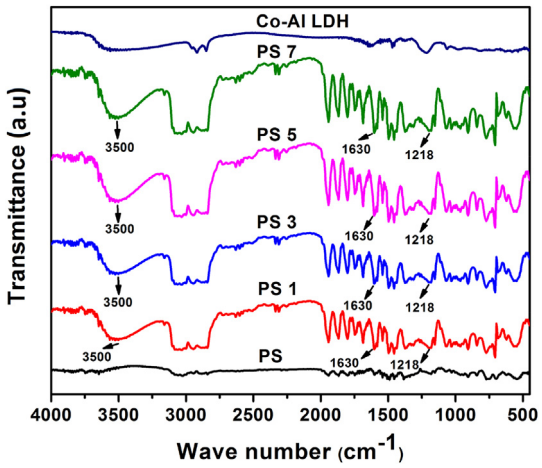

Fig. 5. FTIR spectra of Co–Al LDH, pristine PS and PS/Co–Al LDH nanocomposite samples.

3.4. Thermal properties

3.4.1. TGA analysis

TGA analysis is primarily utilized to examine the degradation temperature as well as thermal stability of the polymer matrix. The TGA curve of Co–Al LDH, pristine PS and its PS/LDH nanocomposites are presented in Fig. 6. TGA profile of Co–Al LDH shows a complex thermal degradation behavior. For Co–Al LDH ((Fig. 6 (a)), the mass loss before 200 °C is attributed to the loss of physically adsorbed and interlayer water [2]. The mass loss between 200 and 350 °C corresponds to the decomposition of the interlayer dodecyl sulfate [24]. The mass loss above 350 °C is attributed to the decomposition of LDH sample up to the formation of Co–Al oxides. The main degradation of pristine PS takes place in the temperature range of 350–450 °C (see Fig. 6 (b)) In the case of PS/LDH nanocomposites, two types of degradation profile are observed. The first stage of weight decrement at 140–330 °C is due to the vaporization of physisorbed water molecules in the intercalated galleries and the thermal degradation of alkyl chains of surfactant molecules [12]. The second stage decrement at 330–460 °C is due to the thermal decomposition of PS macromolecules and the creation of black char. Only inorganic residues are present beyond the temperature of 460 °C. From these TGA results, it is evident that the thermal stability of the PS nanocomposites is enhanced by the incorporation of LDH nanofiller. This is attributed to the barrier effect of LDH layers that hinders the heat and the diffusion of volatile components generated by thermal degradation. Considering mass decrement of 15% as a reference point, the decomposition temperature (T_d) for pristine PS and PS/Co–Al LDH nanocomposites containing 1, 3, 5 and 7 wt.% of LDH is found to be 360, 370.5, 378.2, 384.6 and 388.5 °C, respectively. The T_d value for PS/Co–Al LDH samples with 1, 3, 5 and 7 wt.% LDH loading is 10.5, 18.2, 24.6 and 28.5 °C higher in comparison with pristine PS, respectively (see Table 2). Among the investigated nanocomposites, the nanocomposite with 7 wt.% LDH content has better thermal stability. This finding clearly signify that the improvement in thermal stability is observed even with small (1 wt.%) addition of LDH and the effect is more pronounced in the nanocomposites samples with higher loading of LDH (>5 wt.%) [23]. It is also noticed from the Fig. 6(c–f), that the char residue of nanocomposites gradually increases with increasing the concentration of LDH in the polymer matrix [25]. Interestingly, similar trend was noticed for PS/O-laponite nanocomposites by Paul and co-workers [11]. In their work, thermal stability enhanced gradually in the case of PS/O-laponite composites with an increment in the nanofiller loading. It is noteworthy to mention that the addition of Co–Al LDH in polyurethane (PU) [9] and polycaprolactone/(PCL) [13] decreased the thermal stability of the polymer. However, in the present work, the thermal stability of the PS is enhanced by 28.5 °C with the addition of 7 wt.% Co–Al LDH content. This improvement is significantly higher than that of any other polymer/Co–Al LDH systems [9,13,14].

In the first derivative of TGA graph (Fig. 7), the peaks indicate the temperature corresponding to the maximum rate of mass decrement (T_{max}). It is apparent that all the derivative curves of the nanocomposites (T_{max}) are shifted to the right hand side of pristine PS, which represents better thermal stability of the composites. The T_{max} value of pristine PS is 417 °C and PS 7 nanocomposite is 424.5 °C, indicating 7.5 °C enhancement with only 7 wt.% of LDH content. Table 2 presents the TGA results of pristine PS and its nanocomposites.

Generally around 10–30 wt.% of inorganic materials such as glass fiber used to reinforce the polymer in order to enhance the properties of the polymer [26]. Nevertheless, it is noticed that a small quantity (even 1 wt.%) of LDH is sufficient to augment the properties of PS due to molecular level dispersion as well as high aspect ratio of the LDH. It is well documented in the literature [27] that the effect of improving the properties increases when the aspect ratio of the filler increases.

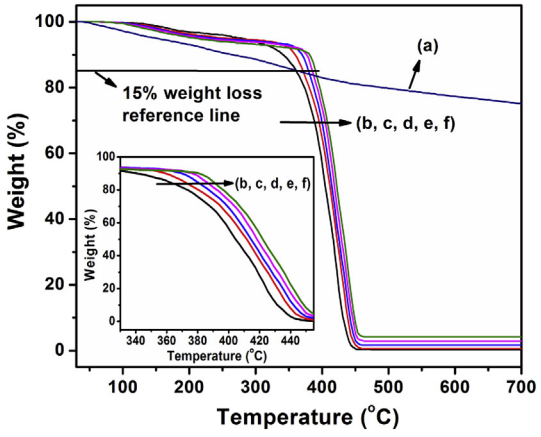

Fig. 6. TGA profiles of (a) Co–Al LDH, (b) PS, (c) PS 1, (d) PS 3, (e) PS 5 and (f) PS 7 nanocomposites (Inset shows the TGA profiles between 330 and 460 °C).

Table 2
Thermal degradation temperatures of PS and PS/Co–Al LDH nanocomposites.

Sample	Temperature at 15% weight loss (T_{15}) °C	$\Delta T_{15\%}$ (°C)	T_{max} (°C)
PS	360.0	–	417.0
PS 1	370.5	10.5	419.9
PS 3	378.2	18.2	422.4
PS 5	384.6	24.6	423.9
PS 7	388.5	28.5	424.5

3.4.2. DSC analysis

To examine the movement of PS macromolecular chains in the clay galleries in term of its glass transition temperature (T_g), DSC analysis of PS/LDH nanocomposites and PS sample without LDH was performed and the obtained results are presented in Fig. 8. The T_g is evaluated at the inflection point between the onset and the end set temperatures. The T_g value is found to be 69.3, 71.8, 73.3, 74.4 and 74.8 °C, for pristine PS, PS 1, PS 3, PS 5, PS 7 sample, respectively. The highest enhancement of T_g (5.5 °C more than pristine PS) is achieved with PS nanocomposite containing 7 wt.% Co–Al LDH content. As a whole, the T_g of PS is improved with the

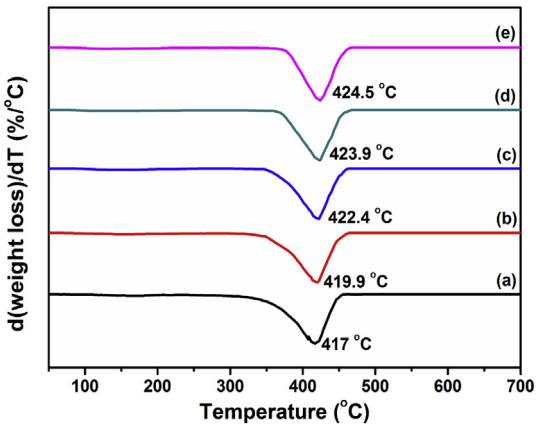

Fig. 7. TGA derivatives of (a) pristine PS, (b) PS 1, (c) PS 3, (d) PS 5, (e) PS 7 nanocomposites.

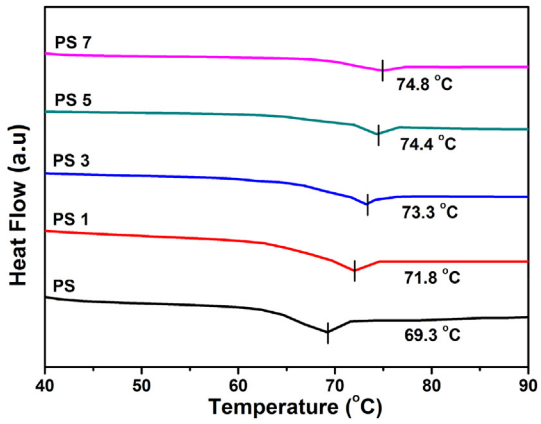

Fig. 8. DSC analysis of pristine PS and PS nanocomposites.

addition of LDH. This is due to the strong linkages between Co–Al LDH and PS, which hinders the supportive movement of the PS primary chain fragments. Similar phenomenon was also observed for PS/O-laponite nanocomposites by Paul and co-workers [11].

3.5. Coats-Redfern method for kinetic analysis

Coats-Redfern [28] method, also called as integral method, is generally applied to study the kinetics of solid state system. The thermal degradation kinetics is studied using following equations:

$$Y = \ln\left(-\frac{\ln(1-\alpha)}{T^2}\right) = \ln\left[\frac{AR}{\beta E_a}\left(1-\frac{2RT}{E_a}\right)\right] - \frac{E_a}{RT} \quad ;\text{for } n = 1 \tag{1a}$$

$$Y = \ln\left(\frac{1-(1-\alpha)^{1-n}}{(1-n)T^2}\right) = \ln\left[\frac{AR}{\beta E_a}\left(1-\frac{2RT}{E_a}\right)\right] - \frac{E_a}{RT} \quad ;\text{for } n \neq 1 \tag{1b}$$

Here, n represents order of reaction, A indicates pre-exponential factor, T denotes the temperature, R represents gas constant, E_a refers to activation energy, and β represents the heating rate. Usually, the logarithmic term on the right hand side of eq. (1) can be considered as constant. The order of reaction (n) is evaluated by linear fitting of the left hand side (Y) of eq. (1) versus 1/T. The value of n obtained at the best correlation coefficient (R) is the actual order of reaction, and E_a and A can also be evaluated.

Coats-Redfern method deals with the major decomposition stage of the thermal behavior of the PS nanocomposites. The thermal degradation data at a single heating rate is sufficient to calculate the respective parameters (A, E_a, and n). Initially, it is assumed that a thermal decomposition reaction comprises a specific order of reaction and it is substituted in eq. (1). To evaluate the best correlation coefficient (R), the graph of left hand side (Y) of eq. (1) is fitted against to 1/T. The stated route is replicated to obtain the best R value. Consequently, A and E_a are evaluated from the intercept and slope of the plotted linear line, respectively. Fig. 9 illustrates the linearly fitted plot of pristine PS and various PS nanocomposites. The obtained kinetic parameter values including n, E_a and A for the prepared samples are enlisted in Table 3. The E_a of pristine PS, PS 1, PS 3, PS 5 and PS 7 nanocomposites is determined as 89, 109, 126, 134 and 138 kJ/mol, respectively. The E_a of PS 7 is found to be 49 kJ/mol higher than the pristine PS (see Table 3). Chen and Wang [18] also showed an enhancement in E_a for PP nanocomposites in comparison with pristine polymer.

3.6. Criado method for the reaction mechanism analysis

The degradation reaction mechanism was evaluated by Criado model with the help of kinetic variables (A, E_a, and n) obtained from Coats-Redfern method [29]. This method can precisely find out the reaction mechanism in the solid reactions. This is defined by a $Z(\alpha)$ type function.

$$Z(\alpha) = \frac{\beta}{A} g(\alpha) \frac{d\alpha}{dt} e^{\frac{E_a}{RT}} \tag{2a}$$

$$Z(\alpha) = \frac{d\alpha}{dt} \frac{E_a}{R} e^{\frac{E_a}{RT}} P(x) \tag{2b}$$

The master Z(α)-α curve can be plotted using Eq. (2a) according to the various reaction mechanisms, reported in details elsewhere [30]. The Eq. (2b) is used to plot the experimental Z(α)-α curve. By comparing these two curves, the type of mechanism involved in the thermal degradation process can be identified. The Z(α)-α master and experimental curve of pristine PS and its nanocomposites is shown in Fig. 10. It is apparent that the pristine PS nearly follows the the master curve of $Z(F_1)$, demonstrating that the thermal decomposition process of pristine PS is associated to F1 reaction mechanism. According to literature, this degradation mechanism refers to random nucleation with one nucleus on the individual particle [30]. In this type of mechanism, the degradation is initiated from random points, which act as growth center for the progress of the degradation reaction. After adding Co–Al LDH, for all PS/Co–Al LDH nanocomposites samples, involved system holds F1 reaction mechanism at lower α value ($\alpha = 0.15–0.4$). Nevertheless, at higher conversion ($\alpha = 0.7–0.9$), the development of the thermal degradation reaction tends towards A4 mechanism, which corresponds to nucleation and growth.

3.7. Integral procedural decomposition temperature

To evaluate the nanocomposites thermal stability, integral procedural decomposition temperature (IPDT) method was employed by considering the overall shape of the TGA curve. According to Doyle's method [31], the estimation of IPDT value is done using the following expression:

$$\text{IPDT}(^\circ\text{C}) = K \times S \times \left(T_f - T_i\right) + T_i \tag{3}$$

where, $S = (A_1+A_2)/(A_1+A_2+A_3)$; $K = (A_1+A_2)/(A_1)$; S is the area ratio of total experimental curve specified by the total TGA thermogram. T_f and T_i are the final and initial experimental temperature. As shown in Fig. 11, A_1, A_2, and A_3 are partition of three different areas of the typical TGA thermogram graph. For all the prepared samples, the IPDT values are determined using Eq. (3). The IPDT values of pristine PS and PS/Co–Al LDH nanocomposites containing 1, 3, 5 and 7 wt.% of LDH is found to be 380.4, 388.5, 402.6, 410.7 and 415.8 °C, respectively (see Table 3). As expected, the IPDT value of nanocomposites increases with increasing LDH concentration, which confirms the increment of thermal stability of nanocomposites. The IPDT value of PS 7 is higher than that of other samples indicating better thermal stability. Similarly, Kim et al. [32] showed the enhancement in IPDT values for nanocomposites over pristine polymer.

3.8. Rheological properties

3.8.1. Storage modulus

Rheological analysis of the polymer composites is very effective tool to study the variation of microstructure and an

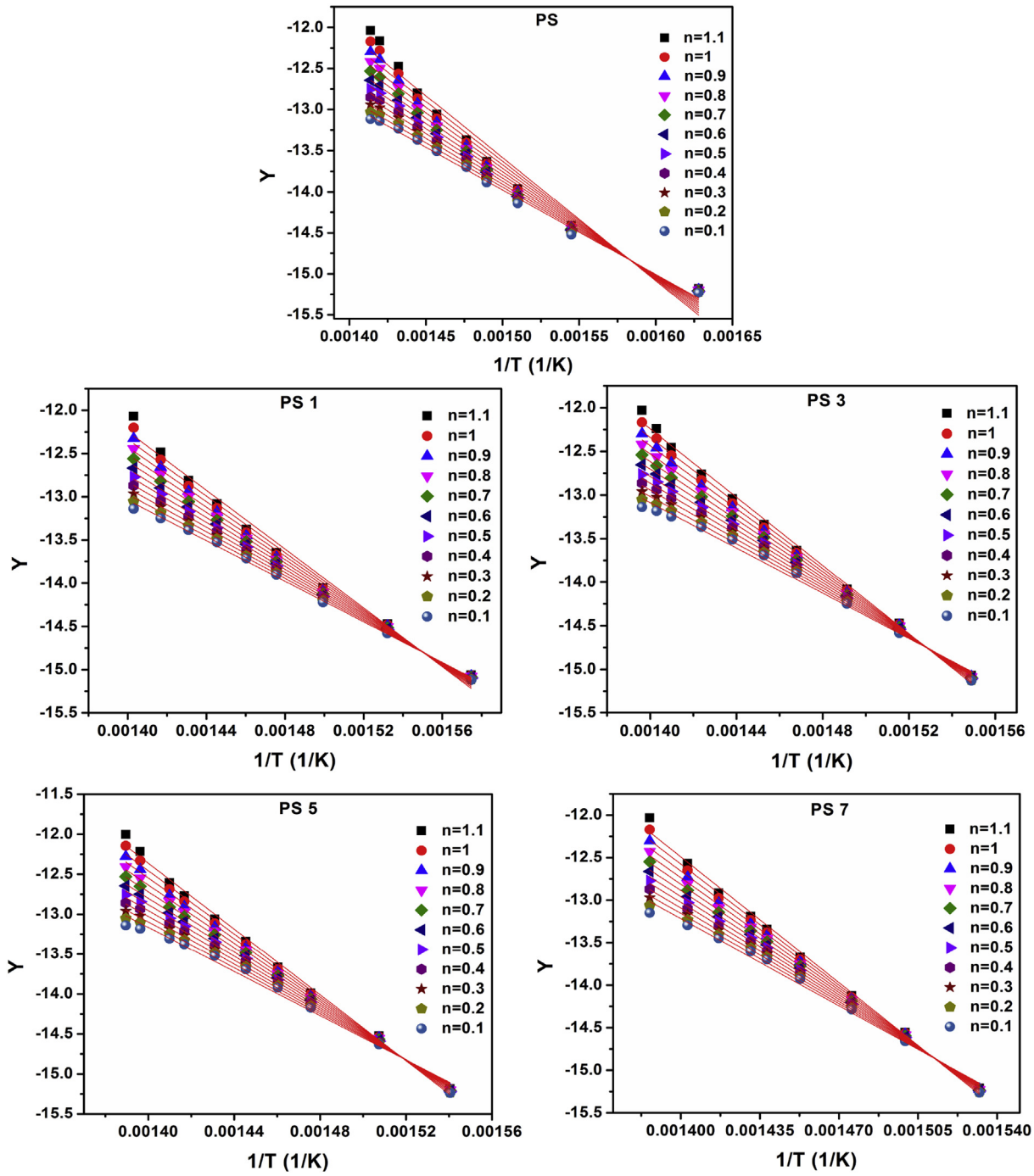

Fig. 9. Determination of kinetic parameters by plots of the left part in eq. (1) against 1/T using Coats-redfern methods.

Table 3
Thermal degradation kinetics of pristine PS and PS/Co–Al LDH nanocomposites obtained from Coats-Redfern method.

Sample	E_a(kJ/mol)	A	n	R^2	IPDT (°C)
PS	89	8.88×10^5	0.2	0.993	380.4
PS 1	109	5.09×10^7	0.5	0.998	388.5
PS 3	126	6.19×10^8	0.5	0.998	402.6
PS 5	134	2.84×10^9	0.5	0.997	410.7
PS 7	138	4.05×10^9	0.5	0.997	415.8

interactive force between the polymer and nanofiller. The analysis was done with varying frequency between 0.01 and 100 s^{-1} at a constant temperature of 190 °C (see Fig. 12). As evident in Fig. 12, the storage modulus of pristine PS is the lowest among all the nanocomposite samples in the entire range of frequency and the storage modulus also increases with increasing LDH concentration. The increase of storage modulus at lower frequency is the characteristic of pseudo-solid like behavior due to the formation of network percolating LDH lamellae. At higher frequency value of 100 sec^{-1}, the storage modulus curves overlap with each other for all the nanocomposite samples. The increment of filler content in the nanocomposites makes it from liquid-like nature to solid-like

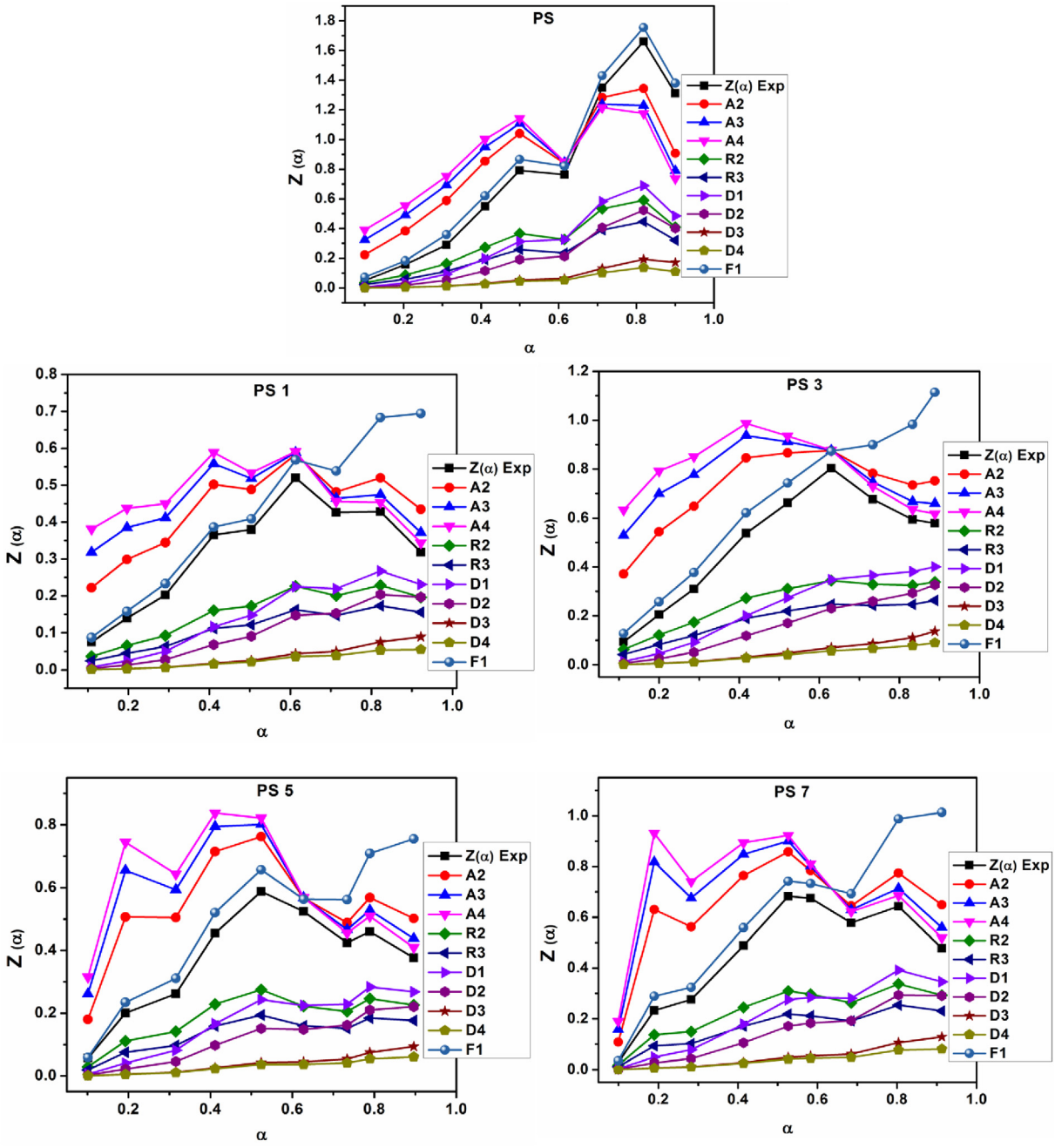

Fig. 10. Determination of the thermal degradation mechanism by plotting Z(α) versus α using Criado model.

nature. This transition concentration is called the rheological percolation threshold. The appearance of rheological percolation threshold in the nanocomposite samples can be attributed to the formation of continuous network of LDH and polymer chain. The same phenomena have been reported for PE/Mg–Al LDH nanocomposites [33] and polymer/layered silicate nanocomposites [34].

3.8.2. Loss modulus

The rheological parameter used to indicate the viscous effect of the given viscoelastic material is 'loss modulus'. Fig. 13 shows the plot of loss modulus versus frequency in the range of 0.01–100 s^{-1} at a temperature of 190 °C. On comparison with the storage moduli of samples, it is apparent that the loss modulus is always higher than the storage modulus at lower frequency indicating the dominance of the viscous part. In the lower frequency region, the rise of loss modulus for the nanocomposite samples is more than the increase observed at higher frequency region, despite the fact that the nature of all the curves is similar. It is apparent that with the addition of LDH, the loss modulus is altered especially at lower frequency region, since it is quite resistive to flow [33]. In the higher frequency region, the relaxation time for the polymer nanocomposites is reduced. It signifies a more flowing situation, which cancels out the resistance caused by LDH and the curves come closer to that of pristine PS.

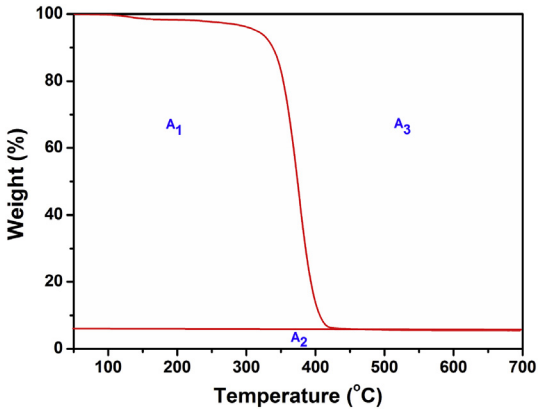

Fig. 11. Schematic diagram of Doyle's method for determining IPDT.

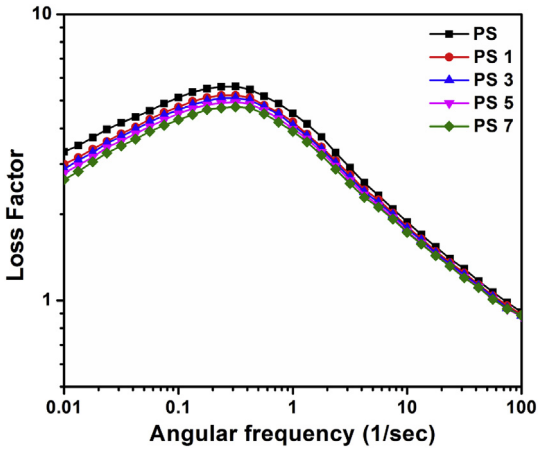

Fig. 14. Loss factor versus angular frequency of pristine PS and its nanocomposites.

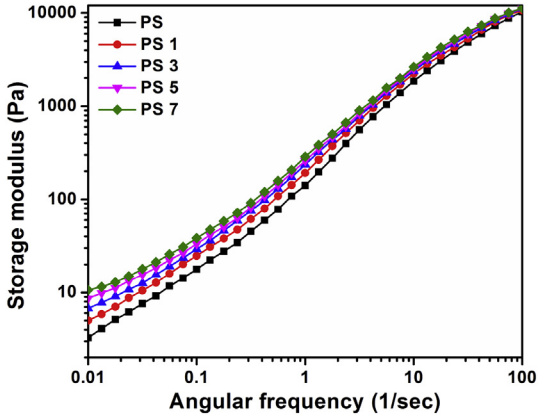

Fig. 12. Storage modulus versus angular frequency of pristine PS and its nanocomposites.

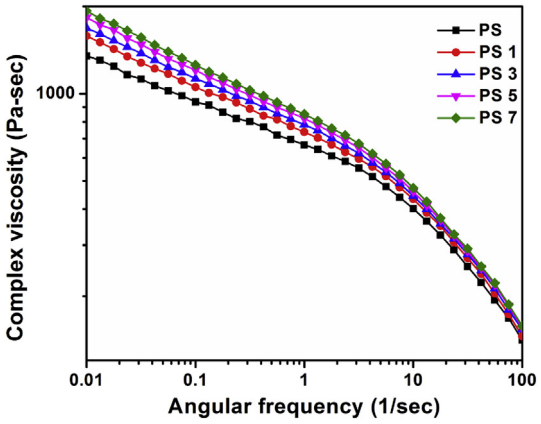

Fig. 15. Complex viscosity versus angular frequency of pristine PS and its nanocomposites.

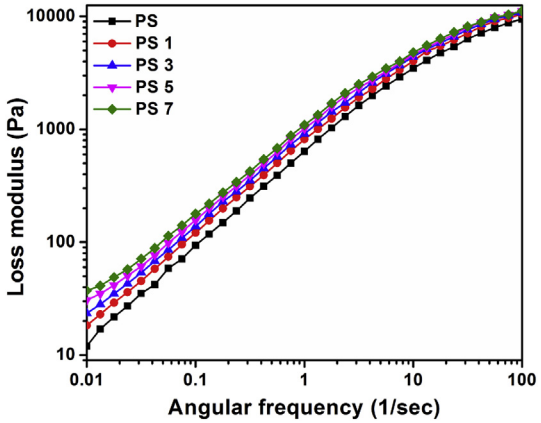

Fig. 13. Loss Modulus versus angular frequency of pristine PS and its nanocomposites.

3.8.3. Loss factor

Fig. 14 shows the loss factor as a function of frequency in the range of 0.01–100 s^{-1} at 190 °C. It is observed that the loss factor of the nanocomposites is lower than that of pristine PS and decreases with increasing LDH concentration in the polymer matrix. This is due to the fact that elastic nature of the nanocomposites increases with increasing the LDH content [33]. Majid et al. [35] also obtained a similar trend of loss factor for PP nanocomposites with ZnO nanofiller.

3.8.4. Complex viscosity

Fig. 15 portrays the behavior of complex viscosity with angular frequency in the range of 0.01–100 s^{-1} at 190 °C. The nanocomposites show a rise in complex viscosity values with increasing the concentration of LDH in the lower frequency region, which is slowly quenched as the frequency increases. The primary cause for this trend is the adhesion between the LDH and PS and the cohesive interactions in the LDH layers. This also explains that the addition of LDH influences more frictional interactions. A transition from Newtonian behavior to a shear thinning nature is also observed with increasing frequency. This is due to the fact that polymer chains have less time to entangle and the direction of randomly dispersed nanofiller is also turned according to the macromolecular chains at higher frequency. As a result, PS nanocomposites are move to near PS curve and all samples exhibit similar trend at higher frequency.

4. Conclusions

The current investigation successfully demonstrated the fabrication of Co–Al LDH based PS nanocomposites with improved

thermal properties via simple solvent blending method. XRD profiles of PS nanocomposites showed no diffraction peak corresponding to basal plane (003) of Co–Al LDH, indicating the formation of exfoliated nanocomposite. TEM micrographs exhibited that the Co–Al LDH platelets were disseminated well within PS matrix. The FTIR results verified the existence of Co–Al LDH in the PS nanocomposites. The DSC results revealed a noticeable improvement in glass transition temperature with the addition of LDH in PS matrix.

TGA results demonstrated that the thermal stability of PS/Co–Al LDH nanocomposites was considerably increased as compared to pristine PS. When 15% mass loss was considered as a point of reference, the thermal decomposition temperature of PS nanocomposites was 10–28.5 °C higher than the pristine PS. The activation energy of PS/Co–Al LDH nanocomposites is about 20–49 kJ/mol higher than that of pristine PS. The obtained IPDT and activation energy data completely correlated with the improvement of the thermal stability of the PS nanocomposites with LDH concentration evidenced by TGA analysis. The findings of thermal degradation kinetics clearly indicated that the nanocomposites initially followed F1 reaction mechanism (random nucleation with one nucleus on the individual particle), while thermal decomposition proceeds, the reaction mechanism shifted to A_4 mechanism (nucleation and growth). The results of rheological analysis revealed that the storage modulus and loss modulus increased as content of LDH increased and also less dependent at higher frequency for a fixed temperature.

Acknowledgement

Authors are grateful to Central Instruments Facility, Indian Institute of Technology Guwahati for their help in performing TEM characterization. XRD utilized in this study was financed by a FIST grant (SR/FST/ETII-028/2010) from the Department of Science and Technology (DST), Government of India.

Nomenclature

θ	Angle of diffraction
λ	Cu-Kα radiation wavelength
T_d	Decomposition temperature
T_{max}	Maximum degradation temperature
T_g	Glass transition temperature
α	Fractional conversion
β	Rate of heating
R	Universal gas constant
E_a	Activation energy
A	Pre-exponential factor
n	Order of reaction
t	Thermogravimetric analysis reaction time
T_f	Final temperature of thermal degradation reaction
T_i	Initial temperature of thermal degradation reaction
S	Thermogram area ratio
K	Thermogram area ratio coefficient
G'	Storage modulus
G''	Loss modulus
η	Complex viscosity
ω	Angular frequency

References

[1] F.R. Costa, A. Leuteritz, U. Wagenknecht, D. Jehnichen, L. Haubler, G. Heinrich, Intercalation of Mg-Al layered double hydroxide by anionic surfactants: preparation and characterization, Appl. Clay Sci. 38 (2008) 153–164.
[2] A.M. Alansi, W.Z. Alkayali, M.H. Al-qunaibit, T.F. Qahtan, T.A. Saleh, Synthesis of exfoliated polystyrene/anionic clay MgAl-Layered double hydroxide: structural and thermal properties, RSC Adv. 5 (2015) 71441–71448.
[3] S.S. Ray, M. Okamoto, Polymer/layered silicate nanocomposites: a review from preparation to processing, Prog. Polym. Sci. 28 (2003) 1539–1641.
[4] R.A. Vaia, K.D. Jandt, E.J. Kramer, E.P. Giannelis, Microstructural evolution of melt intercalated polymer-organically modified layered silicates nanocomposites, Chem. Mater. 8 (1996) 2628–2635.
[5] Y.K. Kim, Y.S. Choi, K.H. Wang, I.J. Chung, Synthesis of exfoliated PS/Na-MMT nanocomposites via emulsion polymerization, Chem. Mater. 14 (2002) 4990–4995.
[6] J. Zhu, A.B. Morgan, F.J. Lamelas, C.A. Wilkie, Fire Properties of polystyrene-clay nanocomposites, Chem. Mater. 13 (2001) 3774–3780.
[7] C. Park, O.O. Park, J.G. Lim, H.J. Kim, The fabrication of syndiotactic polystyrene/organophilic clay nanocomposites and their properties, Polymer 42 (2001) 7465–7475.
[8] Z. Liu, R. Ma, M. Osada, N. Iyi, Y. Ebina, K. Takada, T. Sasaki, Synthesis, anion exchange, and delamination of Co-Al layered double hydroxide: assembly of the exfoliated nanosheet/polyanion composite films and magneto-optical studies, J. Am. Chem. Soc. 128 (2006) 4872–4880.
[9] S. Guo, C. Zhang, H. Peng, W. Wang, T. Liu, Structural characterization, thermal and mechanical properties of polyurethane/CoAl layered double hydroxide nanocomposites prepared via in situ polymerization, Compos. Sci. Technol. 71 (2011) 791–796.
[10] L. Qiu, W. Chen, B. Qu, Structural characterization and thermal properties of exfoliated polystyrene/ZnAl layered double hydroxide nanocomposites prepared via solution intercalation, Polym. Degrad. Stab. 87 (2005) 433–440.
[11] P.K. Paul, S.A. Hussain, D. Bhattacharjee, M. Pal, Preparation of polystyrene-clay nanocomposite by solution intercalation technique, Bull. Mater. Sci. 36 (2013) 361–366.
[12] R. Botan, T.R. Nogueira, F. Wypych, L.M.F. Lona, In situ synthesis, morphology, and thermal properties of polystyrene-MgAl layered double hydroxide nanocomposites, Polym. Eng. Sci. 52 (2012) 1754–1760.
[13] H. Penga, Y. Han, T. Liu, W.C. Tjiu, C. He, Morphology and thermal degradation behavior of highly exfoliated CoAl-layered double hydroxide/polycaprolactone nanocomposites prepared by simple solution intercalation, Thermochim. Acta 502 (2010) 1–7.
[14] M. Kumar, V. Chaudhary, K. Suresh, G. Pugazhenthi, Synthesis and characterization of exfoliated PMMA/Co-Al LDH nanocomposites via solvent blending technique, RSC Adv. 5 (2015) 39810–39820.
[15] S. Limpanart, S. Khunthon, P. Taepaiboon, P. Supaphol, T. Srikhirin, W. Udomkichdecha, Y. Boontongkong, Effect of the surfactant coverage on the preparation of polystyrene-clay nanocomposites prepared by melt intercalation, Mater. Lett. 59 (2005) 2292–2295.
[16] W.A. Zhang, D.Z. Chen, H.Y. Xu, X.F. Shen, Y.E. Fang, Influence of four different types of organophilic clay on the morphology and thermal properties of polystyrene/clay nanocomposites prepared by using the γ-ray irradiation technique, Eur. Polym. J. 39 (2003) 2323–2328.
[17] P. Uthirakumar, M.K. Song, C. Nah, Y.S. Lee, Preparation and characterization of exfoliated polystyrene/clay nanocomposites using a cationic radical initiator-MMT hybrid, Eur. Polym. J. 41 (2005) 211–217.
[18] Y. Chen, Q. Wang, Thermal oxidative degradation kinetics of flame-retarded polypropylene with intumescent flame-retardant master batches in situ prepared in twin-screw extruder, Polym. Degrad. Stab. 92 (2007) 280–291.
[19] S.O. Leary, D.O. Hare, G. Seeley, Delamination of layered double hydroxides in polar monomers: new LDH-acrylate nanocomposites, Chem. Commun. 14 (2002) 1506–1507.
[20] F. Lv, Y. Wu, Y. Zhang, J. Shang, P.K. Chu, Structure and magnetic properties of soft organic ZnAl-LDH/polyimide electromagnetic shielding composites, J. Mater. Sci. 47 (2012) 2033–2039.
[21] B. Du, Z. Guo, Z. Fang, Effects of organo-clay and sodium dodecyl sulfonate intercalated layered double hydroxide on thermal and flame behavior of intumescent flame retarded polypropylene, Polym. Degrad. Stab. 94 (2009) 1979–1985.
[22] A.B. Morgan, J.W. Gilman, Characterization of polymer layered silicate (clay) nanocomposites by transmission electron microscopy and X-ray diffraction: a comparative study, J. Appl. Polym. Sci. 87 (2003) 1329–1338.
[23] H.W. Wang, K.C. Chang, J.M. Yeh, S.J. Liou, Synthesis and dielectric properties of polystyrene-clay nanocomposite materials, J. Appl. Polym. Sci. 91 (2004) 1368–1373.
[24] W. Xie, Z. Gao, K. Liu, W.P. Pan, R. Vaia, D. Hunter, A. Singh, Thermal characterization of organically modified montmorillonite, Thermochim. Acta 367–368 (2001) 339–350.
[25] T. Lan, T.J. Pinnavaia, Clay-Reinforced epoxy nanocomposites, Chem. Mater. 6 (1994) 2216–2219.
[26] T.P.S. Kumar, S.S. Kumar, J. Naveen, Glass fiber-reinforced polymer composites-a review, J. Reinf. Plast. 33 (2014) 1258–1275.
[27] K. Yano, A. Usuki, A. Okada, Synthesis and properties of polyimide-clay hybrid films, J. Polym. Sci. Part A Polym. Chem. 35 (1997) 2289–2294.
[28] A.W. Coats, J.P. Redfern, Kinetic parameters from thermogravimetric data, Nature 201 (1964) 68–69.
[29] J.M. Criado, J. Malek, A. Ortega, Applicability of the master plots in kinetic analysis of non-isothermal data, Thermochim. Acta 147 (1989) 377–385.

[30] S. Ma, J.O. Hill, S. Heng, A kinetic analysis of the pyrolysis of some australian coals by non-isothermal thermogravimetry, J. Therm. Anal. Calorim. 37 (1991) 1161–1177.
[31] C.D. Doyle, Estimating thermal stability of experimental polymers by empirical thermogravimetric analysis, Anal. Chem. 33 (1961) 77–79.
[32] J.Y. Kim, H.J. Choi, C.S. Kang, S.H. Kim, Influence of modified carbon nanotube on physical properties and crystallization behavior of poly(ethylene terephthalate) nanocomposite, Polym. Compos. 31 (2010) 858–869.
[33] F.R. Costa, U. Wagenknecht, D. Jehnichen, G. Heinrich, Nanocomposites based on polyethylene and Mg-Al layered double hydroxide: characterization of modified clay, morphological and rheological analysis of nanocomposites, Plast. Rubber Compos. 35 (2006) 139–148.
[34] Y.T. Lim, O.O. Park, Phase morphology and rheological behavior of polymer/layered silicate nanocomposites, Rheol. Acta 40 (2001) 220–229.
[35] M. Majid, E.D. Hassan, A. Davoud, M. Saman, A study on the effect of nano-ZnO on rheological and dynamic mechanical properties of polypropylene: experiments and models, Compos. Part B 42 (2011) 2038–2046.